

Efficient ground state preparation in variational quantum eigensolver with symmetry-breaking layers

Chae-Yeun Park^{1,2}

¹*Xanadu, M5G 2C8 Toronto, Canada*

²*Institute for Theoretical Physics, University of Cologne, 50937 Köln, Germany*

(*Electronic mail: chae.yeun.park@gmail.com)

(Dated: 31 January 2024)

Variational quantum eigensolver (VQE) solves the ground state problem of a given Hamiltonian by finding the parameters of a quantum circuit ansatz that minimizes the Hamiltonian expectation value. Among possible quantum circuit ansätze, the Hamiltonian variational ansatz (HVA) is widely studied for quantum many-body problems as the ansatz with sufficiently large depth is theoretically guaranteed to express the ground state. However, since the HVA shares the same symmetry with the Hamiltonian, it is not necessarily good at finding the symmetry-broken ground states that prevail in nature. In this paper, we systematically explore the limitations of the HVA for solving symmetry-broken systems and propose an alternative quantum circuit ansatz with symmetry-breaking layers. With extensive numerical simulations, we show that the proposed ansatz finds the ground state in depth significantly shorter than the bare HVA when the target Hamiltonian has symmetry-broken ground states.

I. INTRODUCTION

Experimental progress in controlling quantum systems has allowed the first quantum computational advantage claim¹ in recent years. This achievement initiated the race between noisy intermediate-scale quantum² (NISQ) computers and the state-of-the-art classical algorithms³. Now, a NISQ device with hundreds of qubits is available⁴, and those devices are expected to solve a practical computational problem beyond the reach of classical computers. Among possible applications, variational quantum eigensolver (VQE)^{5,6} that solves the ground state problem of quantum many-body Hamiltonian has gained lots of attention recently (see Ref. 7 for a recent review).

The VQE combines a parameterized quantum circuit and a classical optimization algorithm: A quantum circuit evaluates the expectation value of the Hamiltonian and its derivatives for the output quantum state, whereas a classical optimizer finds better parameters that minimize the energy. As solving the ground state problem of quantum Hamiltonians is difficult for classical computers, one may easily get a possible advantage of VQEs. Still, it is less understood which ansatz and classical optimizer should be used to solve a given Hamiltonian efficiently.

One of the most widely studied ansätze for solving many-body spin Hamiltonians is the Hamiltonian variational ansatz (HVA)^{8,9}. Inspired by a short-depth quantum algorithm for solving combinatorial optimization problems¹⁰, the HVA is constructed using rotating gates whose generators are the terms of the Hamiltonian, which resembles the Suzuki-Trotter decomposition¹¹. Even though the HVA solves many different Hamiltonians reliably¹²⁻¹⁴, however, it is not necessarily good at solving problems with a symmetry-broken nature, which prevails in many-body systems. Indeed, there are local Hamiltonians whose ground states cannot be generated by this ansatz in a constant depth, albeit such a circuit exists, as the circuit obeys the same symmetry as the Hamiltonian¹⁵.

In this paper, we devise a symmetry-breaking ansatz and

explore its power for solving many-body Hamiltonians. We construct our ansatz by adding symmetry-breaking layers to the HVA. The power of those symmetry-breaking ansätze is numerically tested using the transverse-field Ising (TFI) and the transverse-field cluster (TFC) models, which have the \mathbb{Z}_2 and $\mathbb{Z}_2 \times \mathbb{Z}_2$ symmetries, respectively. Our results show that the symmetry-breaking ansatz can find the ground state in a constant depth when the Hamiltonian has symmetry-broken ground states, whereas the bare HVA requires a linear depth for solving the same problem. We also show that, by adding a symmetry penalizing term to the loss function, one can choose a particular symmetry-broken state among degenerate ground states.

II. PRELIMINARIES

A. Hamiltonian variational ansatz

The HVA can be regarded as a parameterized version of the Suzuki-Trotter decomposition. When the Hamiltonian is written as $H = \sum_{i=1}^{\Gamma} h^{(i)}$, the HVA is given by

$$|\psi(\theta)\rangle = \prod_{k=1}^{k=d} \left[\prod_{i=1}^{\Gamma} \exp(-ih^{(i)}\theta_i) \right] |\psi_0\rangle, \quad (1)$$

where $|\psi_0\rangle$ is the ground state of H_0 which is adiabatically connected to H . We note that the HVA is not uniquely defined for a given Hamiltonian, as it depends on how we group the terms of the Hamiltonian. In this paper, we use the most natural construction that groups commuting terms into one generator, i.e., each $h^{(i)}$ has commuting terms. The same construction is also used in Refs. 12 and 14.

For example, let us consider the Hamiltonian of the transverse field Ising (TFI) model for N qubits, which is given by

$$H_{\text{TFI}} = - \sum_{i=1}^N Z_i Z_{i+1} - h \sum_{i=1}^N X_i. \quad (2)$$

For $H_0 = -\sum_i X_i$, an adiabatic path between H_0 and the TFI given by $H(\tau) = (1-\tau)H_0 + \tau H_{\text{TFI}}$ for $0 \leq \tau \leq 1$. As $|+\rangle^{\otimes N}$ is the ground state of H_0 (i.e., at $\tau = 0$), the adiabatic evolution is obtained as follows:

$$|\text{GS}\rangle \approx e^{-i \int_0^T H(t/T) dt} |+\rangle^{\otimes N}. \quad (3)$$

When T is sufficiently larger than $1/(\Delta E)$, where ΔE is the energy gap of the system defined as the difference between the ground and the first excited energies of $H(\tau)$, the adiabatic theorem guarantees that the RHS of Eq. (3) is close to the true ground state of H_{TFI} (i.e., at $\tau = 1$).

We additionally consider the first-order Suzuki-Trotter decomposition of the adiabatic path, which is given by

$$\begin{aligned} & e^{-i \int_0^T H(t/T) dt} |+\rangle^{\otimes N} \\ &= \prod_{k=p}^1 \exp \left[i \left\{ 1 - k\Delta\tau(1-h) \right\} \Delta\tau \sum_{i=1}^N X_i \right] \\ & \quad \times \exp \left[ik\Delta\tau^2 \sum_{i=1}^N Z_i Z_{i+1} \right] |+\rangle^{\otimes N} + O(\Delta\tau), \quad (4) \end{aligned}$$

where $\Delta\tau = 1/p$ and p is the total trotter steps. One can see that p controls both the Trotter error and the error from the adiabatic evolution. Thus, by choosing sufficiently large p , one can find the ground state faithfully.

The HVA is constructed by replacing the Trotter time steps in Eq. (4) with parameters, i.e.,

$$\begin{aligned} & |\psi(\phi, \vartheta)\rangle \\ &= \prod_{k=D}^1 \exp \left[-i\phi_k \sum_{i=1}^N X_i \right] \exp \left[-i\vartheta_k \sum_{i=1}^N Z_i Z_{i+1} \right] |+\rangle^{\otimes N}. \quad (5) \end{aligned}$$

From the above construction, it is clear that the HVA describes the ground state when D is sufficiently large.

However, it is still unclear whether the depth provided by the HVA is optimal (up to a constant factor) for describing the ground state. In this paper, we show that the answer is negative using symmetry-broken systems.

B. Phases related to symmetries

Quantum many-body systems often break a symmetry characterized by a group. When it happens, a system has more than two ground states connected by a group generator. For example, if the \mathbb{Z}_2 symmetry is broken, we can find two ground states $|\text{GS}_0\rangle$ and $|\text{GS}_1\rangle$ such that $|\text{GS}_0\rangle = G|\text{GS}_1\rangle$ where $G \neq \mathbb{1}$ is a generator of this symmetry (or a representation of it, more generally) which satisfies $G^2 = \mathbb{1}$ ^{16,17} (see also Ref. 18 for a general introduction).

Conventionally, the symmetry-breaking phenomena are understood using Landau's theory¹⁹. In this theory, symmetry-broken ground states are determined by an order parameter defined by an expectation value of a local observable O . For the \mathbb{Z}_2 symmetry-broken ground states, one has an order parameter $O_0 = \langle \text{GS}_0 | O | \text{GS}_0 \rangle$ and the other has $O_1 = \langle \text{GS}_1 | O | \text{GS}_1 \rangle = -O_0$. Contrarily, symmetry-preserving ground states have

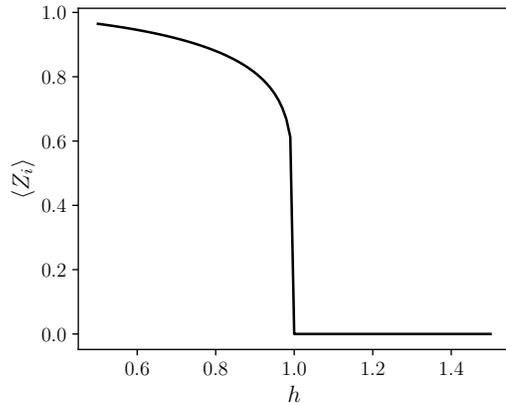


FIG. 1. The order parameter $\langle Z_i \rangle$ as a function of h computed for the ground state of the transverse-field Ising model given by Eq. (2). When $h < 1$, there are two ground states, and the order parameter is computed for one of the ground states. Due to the translational invariance, $\langle Z_i \rangle$ does not depend on i .

$\langle \text{GS} | O | \text{GS} \rangle = 0$. Thus, one can diagnose whether the system breaks the symmetry by computing the order parameter.

A phase transition occurs when the ground state breaks (or restores) a new symmetry as the control parameter of the Hamiltonian changes. For example, the TFI given in Eq. (2) has the strength of the external magnetic field h as a parameter. The Hamiltonian has the \mathbb{Z}_2 symmetry under the spin-flip; it does not change under the transformation $Z_i \leftrightarrow -Z_i$. However, the symmetry of the ground state is broken when $|h| < 1$, i.e., it has two symmetry-broken ground states when $|h| < 1$ in the thermodynamic limit. In Fig. 1, we plot the order parameter $\langle Z_i \rangle$ as a function of h ²⁰ for one of the ground states. One finds that $\langle Z_i \rangle \neq 0$ for $h < 1$, whereas $\langle Z_i \rangle = 0$ for all $h > 1$. This implies that a phase transition occurs at $h = 1$, and the symmetry is broken when $h < 1$.

In general, true symmetry breaking is only observed in the thermodynamic limit, i.e., a system often has a symmetry-preserving unique ground state for any finite N even when it has degenerated ground states in the thermodynamic limit. Thus, we need a diagnostic that can tell whether a system breaks symmetry using the ground states for finite-size systems. Correlation functions are widely used for that purpose. For example, in 1D system, consider local observables $\{O_i\}$ where each O_i supports site i . Then, the correlation function of the ground state is given by $C(i, j) = \langle O_i O_j \rangle - \langle O_i \rangle \langle O_j \rangle$ where $\langle \cdot \rangle$ is the expectation value for the ground state from a system of size N . If $C(i, j)$ converges to a constant as $|j - i| \rightarrow \infty$ (we also need to increase N accordingly), the system has symmetry broken ground states in the thermodynamic limit¹⁸.

With the advent of topological physics^{21–23}, however, systems with degenerate ground states related by a symmetry that an order parameter or correlation functions cannot diagnose are discovered. Such an example includes the AKLT model²⁴, which has been extensively studied over decades. The model has two ground states in the open boundary condition, but the correlation function decays exponentially, and

none of the local observable can distinguish the two states. This type of phase is named symmetry-protected topological (SPT) phase²⁵.

To incorporate both the conventional (symmetry-broken) and the SPT phases under a single theory, a modern definition of quantum phases has been introduced^{26,27}. This theory is technically involved, but in essence, it tells that two Hamiltonians (H_0 and H_1) are in the same phase if there exists a local and gapped parameterized Hamiltonian $H(\tau)$ ($0 \leq \tau \leq 1$) such that $H(0) = H_0$, $H(1) = H_1$ and $H(\tau)$ has the same symmetry for all $0 \leq \tau \leq 1$ (i.e., there exists an operator P such that $[P, H(\tau)] = 0$). Here, we say $H(\tau)$ is gapped when the difference between the lowest and the first-excited eigenvalues of $H(\tau)$ is bounded below by a constant regardless of the system size N . This definition generalizes Landau's theory since the gap closes in the thermodynamic limit during symmetry-breaking phase transitions.

Since adiabatic evolution of a gapped Hamiltonian is described by a constant-depth quantum circuit²⁸, the above definition is directly translated into a language of quantum circuits. Let us assume that Hamiltonians H_0 and H_1 have ground states $|\psi_0\rangle$ and $|\psi_1\rangle$, respectively. Then, $|\psi_0\rangle$ and $|\psi_1\rangle$ are in the same SPT phase if there exists a unitary operator U such that (1) U can be expressed by a local and constant depth quantum circuit, (2) $|\psi_1\rangle = U|\psi_0\rangle$, and (3) $[U, P] = 0$ where P is the symmetry generator.

If we drop the symmetry restriction from the definition of the SPT phases, we arrive at the definition of topological phases²⁹. Namely, two ground states are in different topological phases if we cannot find any local constant-depth circuit U that connects the two states. It is also known that true topological phases do not exist in the one-dimensional spin systems, i.e., one can always find a constant-depth circuit connecting between ground states of any gapped 1D local Hamiltonians^{26,27,30,31}. In the following section, we will use such a distinction between the SPT and topological phases to design an efficient quantum circuit ansatz.

III. SYMMETRY BREAKING ANSATZ

The first model we study is the TFI model for N qubits defined in Eq. (2), where we impose the periodic boundary condition $Z_{N+1} = Z_1$. This model has two distinct (ferromagnetic and paramagnetic) phases depending on the strength of h protected by the spin-flip symmetry $P = \prod_i X_i$ ³². The critical point of this model $h = 1$ is well known²⁰. This implies that if there is a circuit that commutes with P and connects two ground states in different phases (i.e., ground states for $h > 1$ and $h < 1$), the circuit depth must be larger than a constant²⁶. On the other hand, a finite-depth circuit that connects two different ground states exists if we do not restrict such symmetry to a circuit since the system is gapped unless $h = 1$ ^{26,31}.

As the HVA only utilizes terms within the Hamiltonian, it fails to represent such a circuit. To understand this limitation,

let us rewrite the HVA for the TFI given in Eq. (5) as follows:

$$|\psi(\phi, \vartheta)\rangle = \prod_{k=D}^1 [\mathcal{L}_x(\phi_k) \mathcal{L}_{zz}(\vartheta_k)] |+\rangle^{\otimes N} \quad (6)$$

where each layer is given by

$$\mathcal{L}_x(\phi) = \exp[-i\phi \sum_{i=1}^N X_i] \quad (7)$$

$$\mathcal{L}_{zz}(\vartheta) = \exp[-i\vartheta \sum_{i=1}^N Z_i Z_{i+1}]. \quad (8)$$

Let us denote L by the total number of layers, i.e., $L = 2D$ for Eq. (6). As all gates commute with P , i.e. $[P, \mathcal{L}_{zz}] = [P, \mathcal{L}_x] = 0$, and the input state $|+\rangle^{\otimes N}$ is the ground state of the Hamiltonian when $h \rightarrow \infty$, we know that preparing the ground state for $h < 1$ requires circuit depth larger than a constant. Indeed, theoretical and numerical studies have found that this type of ansatz needs depth $D \geq N/2$ to prepare the ground state faithfully^{12,33}.

We now add symmetry-breaking layers in VQE ansatz and see whether it can achieve lower circuit depth for preparing the ground state. Our ansatz for the TFI is given as

$$|\psi(\boldsymbol{\theta})\rangle = \prod_{j=D}^1 \mathcal{L}_z(\phi_j) \mathcal{L}_x(\kappa_j) \mathcal{L}_{zz}(\vartheta_j) |+\rangle^{\otimes N} \quad (9)$$

where $\mathcal{L}_z(\phi_j) = \exp[-i\phi_j \sum_i Z_i]$, and $\boldsymbol{\theta} = \{\vartheta_j, \kappa_j, \phi_j\}_{j=1}^D$ is a set of all parameters. All layers in the ansatz preserve the translational symmetry, but the $\mathcal{L}_z(\phi_j)$ layers break the symmetry P of the Hamiltonian. In addition, as each block now has 3 layers, the total number of layers is $L = 3D$.

Symmetry-preserving/breaking ansätze with the same D [Eqs. (6) and (9)] have different numbers of total gates. However, the number of entangling gates of both circuits is the same. When implemented on NISQ devices, the latter dominates the quality of the output states since the expected fidelity of entangling gates is much lower than single-qubit gates (see, e.g., Refs. 34 and 35). Thus, in the following discussion, we mainly compare the results from these ansätze with the same D .

To observe the effect of symmetry-breaking layers, we simulated the VQE for the TFI using the bare HVA and our symmetry-breaking ansatz given in Eq. (9). We optimize parameters of the ansatz using the quantum natural gradient³⁶⁻³⁸. For each epoch t , we update parameters as $\boldsymbol{\theta}_{t+1} = \boldsymbol{\theta}_t - \eta (\mathcal{F} + \lambda_t \mathbb{1})^{-1} \nabla_{\boldsymbol{\theta}} \langle \psi(\boldsymbol{\theta}_t) | H | \psi(\boldsymbol{\theta}_t) \rangle$ where η is the learning rate, $\mathcal{F} = (\mathcal{F}_{ij})$ is the quantum Fisher matrix, and λ_t is a (step dependent) regularization constant. We choose this optimizer as it works more reliably in solving the ground problem both for classical neural networks³⁹ and VQEs¹³. For the quantum Fisher matrix, we use the centered one $\mathcal{F} = \mathcal{F}_{ij}^c = \Re\{\langle \partial_{\theta_i} \psi(\boldsymbol{\theta}_t) | \partial_{\theta_j} \psi(\boldsymbol{\theta}_t) \rangle - \langle \partial_{\theta_i} \psi(\boldsymbol{\theta}_t) | \psi(\boldsymbol{\theta}_t) \rangle \langle \psi(\boldsymbol{\theta}_t) | \partial_{\theta_j} \psi(\boldsymbol{\theta}_t) \rangle\}$ ³⁷ mostly (unless otherwise stated), but the uncentered one $\mathcal{F}_{ij}^{nc} = \Re\{\langle \partial_{\theta_i} \psi(\boldsymbol{\theta}_t) | \partial_{\theta_j} \psi(\boldsymbol{\theta}_t) \rangle\}$ ³⁶ is also considered when it improves the performance. The difference between

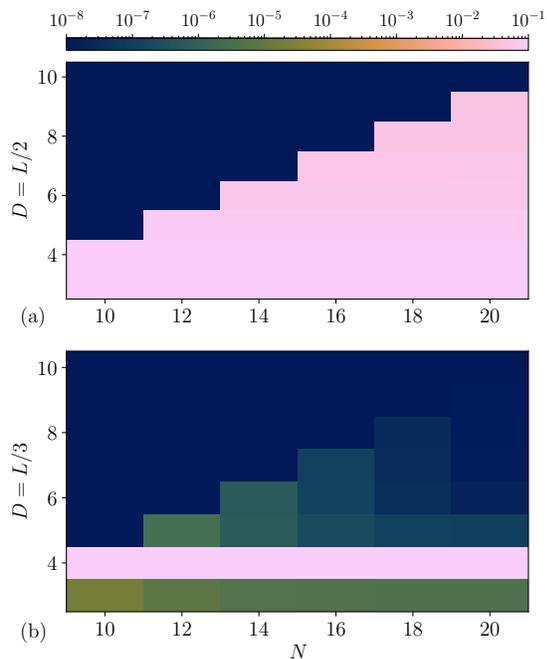


FIG. 2. Converged normalized energy $\tilde{E} = (E_{\text{VQE}} - E_{\text{GS}})/E_{\text{GS}}$ as a function of system size N and the number of blocks D (a) without and (b) with symmetry breaking layers for the transverse field Ising (TFI) model where E_{GS} is the true ground state energy. We have run 12 independent VQE runs and taken the best-optimized energy for each N and D . Initial parameters are sampled randomly from the normal distribution $\mathcal{N}(0, \sigma^2)$ besides $D = 3, 5$ at (b) where we have added $2\pi/D$ to the parameters of the symmetry breaking layers (see main text for details). Note that the total number of layers L is $2D$ for the bare HVA but $3D$ for our symmetry-breaking ansatz.

the two can be understood using the notion of the projected Hilbert space³⁸. For the hyperparameters, we typically use $\eta = 0.01$ and $\lambda_t = \max(100.0 \times 0.9^t, 10^{-3})$.

We present the optimized normalized energies $\tilde{E} = (E_{\text{VQE}} - E_{\text{GS}})/E_{\text{GS}}$ for different N and D in Fig. 2 when $h = 0.5$. We have used the Fisher matrix with the centering term \mathcal{F}^c , and initial values of parameters $\{\vartheta_j, \kappa_j \phi_j\}$ are sampled from the normal distribution $\mathcal{N}(0, \sigma^2)$ with $\sigma = 0.001$ besides $D = 3, 5$ at Fig. 2(b). When $D = 3$ (all N) and 5 (for $N \geq 12$), this initialization does not give any better energy than the ansatz without symmetry-breaking layers. We instead found that initializing parameters for the symmetry breaking layers $\{\phi_j\}$ with samples from $\mathcal{N}(2\pi/D, \sigma^2)$ finds better optima in these cases. However, this initialization does not change the results for $D = 4$ and performs even worse when $D \geq 6$ (see Appendix A for detailed comparisons).

Fig. 2(a) shows that the ground state is only found for $D \geq N/2$ when symmetry-breaking layers are absent, which is consistent with Refs. 12 and 13. On the other hand, results with symmetry-breaking layers [Fig. 2(b)] clearly demonstrate that converged energies are significantly improved for $5 \leq D < N/2$. Most importantly, converged normalized energies are $\leq 10^{-7}$ for all N when $D \geq 9$, which implies that our ansatz finds a constant-depth circuit for solving the ground

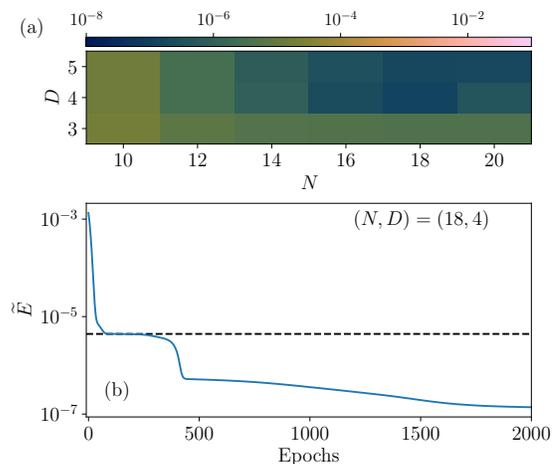


FIG. 3. (a) Converged normalized energies \tilde{E} for system size N and circuit depth D (a) from the transfer learning. Results for $D = 3$ is from the random initialization (which are shown in Fig. 2). For $D = 4$, we have trained a circuit after adding a randomly initialized block in the middle of the converged circuit from $D = 3$ (for the same N). Likewise, we obtained results for $D = 5$ using the converged circuits from $D = 4$. (b) A learning curve from the transfer learning when $(N, D) = (18, 4)$. The dashed line indicates the converged energy from $(N, D) = (18, 3)$.

state. In addition, the results show that there is a finite-size effect up to $N = 18$ where the accurate ground state is only obtained when $D \geq N/2$.

However, the converged energies and the true ground state show a large discrepancy when $D = 4$. In fact, the results for $D = 4$ are even worse than those of $D = 3$, which signals that the optimizer gets stuck in local minima. This type of convergence problem is already observed in Ref. 13. To obtain a better convergence for $D = 4$, we employ a transfer learning technique. Instead of starting from a randomly initialized circuit, we insert a block in the middle of the converged circuit from $D = 3$ and perturb all parameters by adding small numbers sampled from $\mathcal{N}(0, \sigma'^2)$ (where we typically use $\sigma' = 0.01$). We then optimize the full circuit using the quantum natural gradient.

We show converged energies from the transfer learning in Fig. 3. Fig. 3(a) illustrates that the transfer learning succeeds in finding a better optimum for $D = 4$. However, the result for $(N, D) = (10, 5)$ is worse than that of the random initialization, which implies that the transfer learning does not necessarily find the global optima. We additionally plot a learning curve for $(N, D) = (18, 4)$ in Fig. 3(b) where the initial energy is much higher due to an added perturbation but it eventually finds a quantum state with lower energy.

We next consider the transverse-field cluster (TFC) model, the Hamiltonian of which is given as

$$H_{\text{TFC}} = - \sum_{i=1}^N Z_i X_{i+1} Z_{i+2} - h \sum_{i=1}^N X_i. \quad (10)$$

It is known that the phase transition of this model also takes place at $h = 1^{40}$. As the terms $Z_i X_{i+1} Z_{i+2}$ are mutually com-

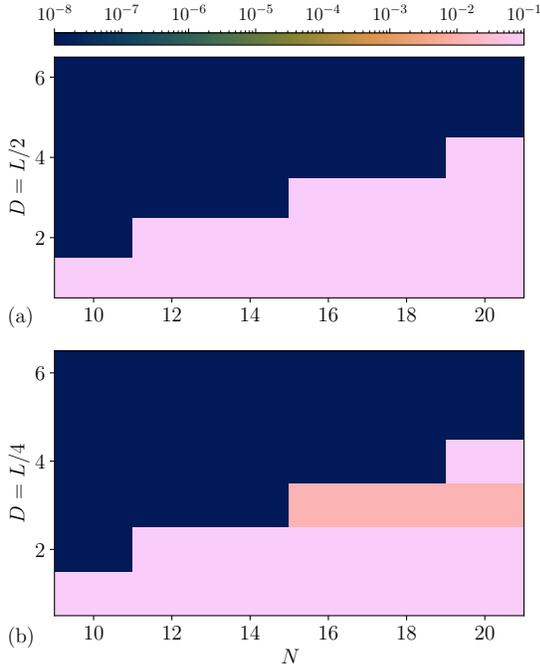


FIG. 4. Converged normalized energies \tilde{E} for system size N and the number of blocks D (a) without and (b) with symmetry breaking layers for the transverse field Cluster (TFC) model.

muting, the ground state at $h = 0$ is the common eigenvector of those operators, which is also known as the cluster state. Two relevant symmetries that determine the ground state of this model are $P_1 = \prod_{i=1}^{N/2} X_{2i}$ and $P_2 = \prod_{i=1}^{N/2} X_{2i-1}$ ^{17,41}. By the definition of SPT, a constant-depth circuit that brings the product state $|+\rangle^{\otimes N}$ to the ground state of the Hamiltonian for $h < 1$ does not exist as long as the circuit commutes with P_1 and P_2 .

We study whether a symmetry-breaking layer can improve it. To see this, we construct our ansatz

$$|\psi(\boldsymbol{\theta})\rangle = \prod_{j=D}^1 \mathcal{L}_z^{\text{even}}(\phi_j) \mathcal{L}_z^{\text{odd}}(\chi_j) \mathcal{L}_x(\kappa_j) \mathcal{L}_{zx}(\theta_j) |+\rangle^{\otimes N} \quad (11)$$

where $\mathcal{L}_{zx}(\theta_j) = \exp[-i\theta_j \sum_{i=1}^N Z_i X_{i+1} Z_{i+2}]$, $\mathcal{L}_z^{\text{even/odd}}(\phi_j) = \exp[-i\phi_j \sum_{i=1}^{N/2} Z_{2i/2i+1}]$. Converged normalized energies with and without symmetry-breaking layers for $h = 0.5$ are shown in Fig. 4. The results without symmetry-breaking layers (without $\mathcal{L}_z^{\text{even/odd}}$) show that circuits with $D \geq \lceil N/4 \rceil$ solve the ground state accurately. However, the symmetry-breaking layers only improve the results for $D = 3$ when $N \geq 16$ for this Hamiltonian. In addition, such an improvement is observed only when the uncentered Fisher matrix \mathcal{F}^{nc} and the initial value $2\pi/D$ for symmetry-breaking layers are used.

In summary, our ansatz does not find a constant-depth circuit for solving the ground state of the TFC based on the results up to $N = 20$. We attribute this to the finite-size effect and

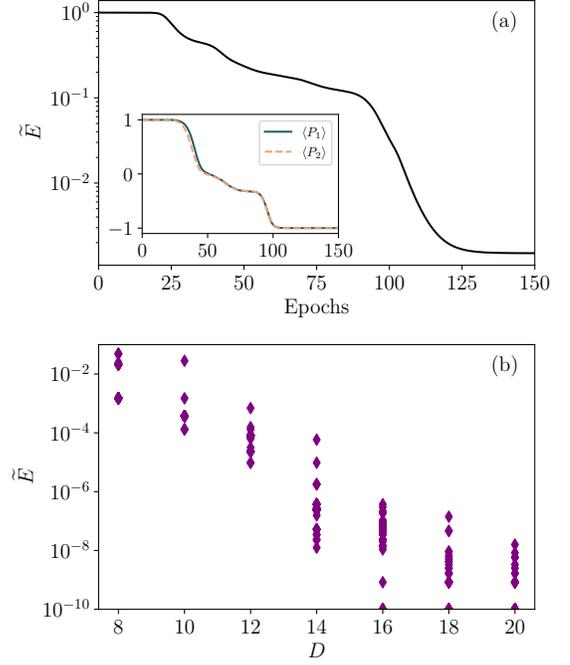


FIG. 5. (a) Learning curve of the VQE for preparing the ground state with $\langle P_1 \rangle = \langle P_2 \rangle = -1.0$. A circuit with $(N, D) = (14, 8)$ is used. Inset shows the learning curves for $\langle P_1 \rangle$ and $\langle P_2 \rangle$. (b) Converged normalized energies \tilde{E} for difference circuit depths D . For each D , we show converged energies from 48 independent VQE runs.

expect that a much larger system size N (beyond our computational capacity) is required to take advantage of symmetry-breaking ansatz.

IV. PREPARING A SYMMETRY BROKEN GROUND STATE

We next consider the cluster Hamiltonian [Eq. (10) with $h = 0$] with the open boundary condition, which is given as

$$H_{\text{cluster}} = - \sum_{i=1}^{N-2} Z_i X_{i+1} Z_{i+2}. \quad (12)$$

Ground states of this model are stabilized by $N - 2$ terms ($Z_i X_{i+1} Z_{i+2} |\psi_{\text{GS}}\rangle = |\psi_{\text{GS}}\rangle$ for $i \in [1, \dots, N - 2]$), so 4-fold degenerate. As the operators P_1 and P_2 commute with all stabilizers, they further define the ground state manifold. For the HVA given in Eq. (11), the output state must be +1 eigenstate of P_1 and P_2 as they commute with the circuit and $P_{1,2} |+\rangle^{\otimes N} = +1 |+\rangle^{\otimes N}$, i.e., it can only find the ground state with $P_1 = P_2 = 1$. In contrast, we show our ansatz [Eq. (11)] (with $\mathcal{L}_{zx}(\theta_j)$ in the open boundary condition) can be used to prepare a particular state within the manifold.

The main idea is minimizing the expectation value of $O = H_{\text{cluster}} + \alpha_1 P_1 + \alpha_2 P_2$ for suitable α_1 and α_2 , instead of the Hamiltonian itself. We expect the obtained state to be an eigenstate with the corresponding eigenvalue ± 1 of P_i when $\text{sign}(\alpha_i) = \mp 1$.

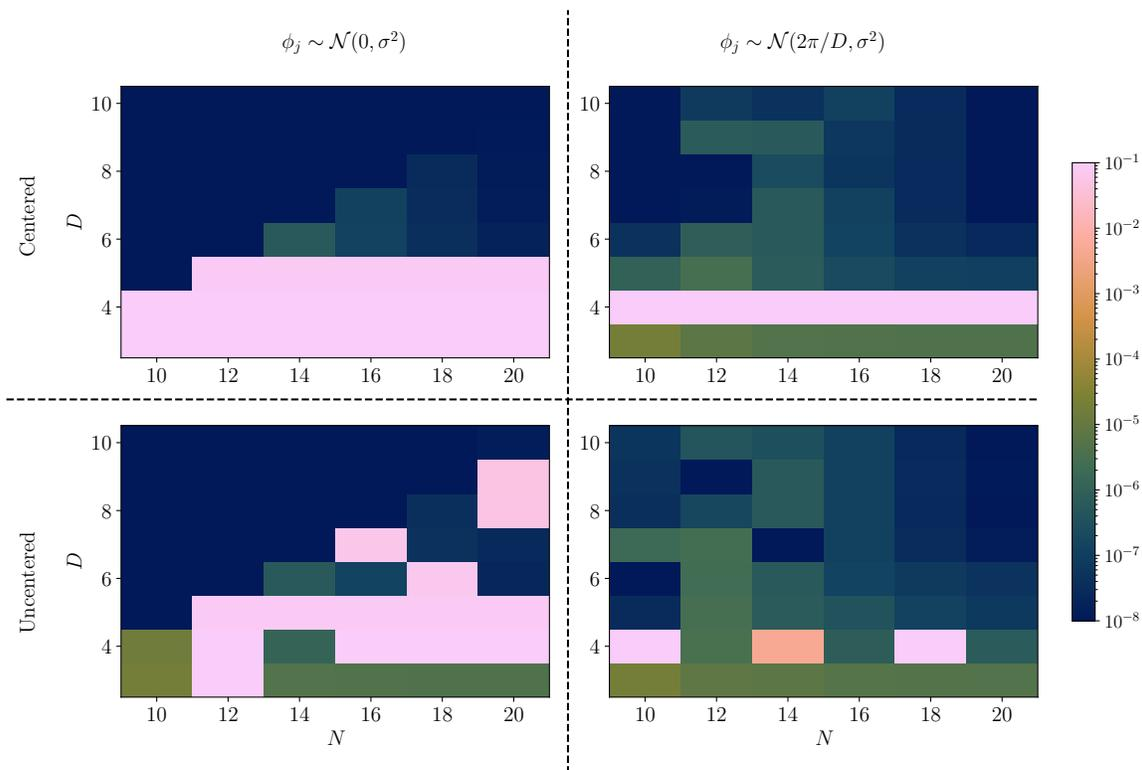


FIG. 6. Converged normalized energies \tilde{E} for the TFI with different optimization set-ups. We have used the centered \mathcal{F}^c and uncentered Fisher matrix \mathcal{F}^{nc} for the upper and lower rows, respectively. The left and right columns show results from different initial values for the symmetry-breaking layers. For each N and D , we have taken the best-optimized energy from 12 independent VQE runs.

For example, we study the VQE for preparing the ground state with $P_1 = P_2 = -1$ using $(N, D) = (14, 8)$. We have tested VQEs with the varying learning rates $\eta \in [0.01, 0.025, 0.05, 0.1]$ and $\alpha_1 = \alpha_2 = \alpha \in [0.1, 0.3, 0.5, 1.0, 2.0, 4.0]$, and found that the desired state can be prepared by the best for $\eta = 0.025$, $\alpha = 2.0$. Especially, all VQE runs have converged to $\langle P_1 \rangle = \langle P_2 \rangle = -1$ (accuracy within 10^{-8}) with these values of η and α . The resulting learning curve is shown in Fig. 5(a). However, the converged energy $\tilde{E} \approx 1.502 \times 10^{-3}$ for $D = 8$ is significantly worse than the results from other models we have studied above (we still note that this is comparable to results from the Adam optimizer which gives normalized energies $\approx 10^{-2} - 10^{-4}$)¹⁴. We thus further study whether increasing D helps the convergence in Fig. 5(b). The results show that the converged energies are getting more accurate as we increase D . Precisely, 47 instances out of 48 independent VQEs runs have converged to $\tilde{E} \leq 10^{-8}$ when $D = 20$. This contrasts the barren plateaus narrative⁴² that more expressive quantum circuits are prone to suffer the optimization problem⁴³. We believe that the behavior of our circuits is related to the known fact in classical machine learning that over-parameterized networks converge better⁴⁴, but we leave a detailed study for future work.

V. CONCLUSION AND OUTLOOK

We studied the limitation of the bare HVA for solving a system with symmetry-broken ground states and proposed an ansatz with symmetry-breaking layers to overcome this problem. Such a symmetry-breaking ansatz could enhance the overall performance of the VQE. Especially for the transverse-field Ising model, we observed that our symmetry-breaking ansatz finds a constant-depth circuit for the ground state, whereas the bare HVA requires the depth to be linear in the system size. We further proposed a technique to choose a specific symmetry broken ground state among possible ground states. This was possible by adding a penalizing term to the cost function.

We expect that one can observe similar behavior for continuous symmetry, e.g., $U(1)$ or $SU(2)$. However, given that those symmetries are not broken in 1D⁴⁵, we should use 2D models to observe the effect of symmetry-breaking layers. Symmetry-broken 2D spin models are also physically interesting as they are related to the lattice gauge theory⁴⁶. However, we leave the detailed study of 2D models for future work, as numerical simulation of such models is more demanding.

Our symmetry-breaking ansatz can be implemented on real quantum hardware. In this case, one should decompose a gate into the set of gates supported by a target quantum device. For example, a gate $\mathcal{L}_{zx}(\theta_j)$, used for the transverse-field cluster model is not naturally supported by most quantum computing

architectures^{47–51,52}. Instead, it can be decomposed into, e.g., $e^{-i\theta Z_{i-1}X_i Z_{i+1}} = CZ_{1,2}CZ_{2,3}e^{-i\theta X_i}CZ_{1,2}CZ_{2,3}$, which may increase overall circuit depths. Still, as our symmetry-breaking ansatz can provide a *scaling* advantage, there is a certain number of qubits that our circuit can solve the problem in a shorter depth than the bare HVA even after such a decomposition.

Incoherent noise can be a significant problem when implemented on noisy quantum hardware. While a weak incoherent noise may help to find a symmetry-broken ground state when the target state is not entangled⁵³, we generally expect that the noise destroys the quantumness of the circuit, and the circuit outputs a decohered state that is far from a true ground state⁵⁴. As the circuit depth is the main factor limited by this type of noise, our symmetry-breaking ansatz may again have an advantage over the bare HVA when the noise is considered.

ACKNOWLEDGMENTS

The author thanks David Wierichs for helpful discussions. This project was funded by the Deutsche Forschungsgemeinschaft under Germany’s Excellence Strategy - Cluster of Excellence Matter and Light for Quantum Computing (ML4Q) EXC 2004/1-390534769 and within the CRC network TR 183 (project grant 277101999) as part of project B01. The numerical simulations were performed on the JUWELS cluster at the Forschungszentrum Juelich.

DATA AVAILABILITY STATEMENT

The source code for the current paper can be found in the Github repository⁵⁵.

Appendix A: Optimization of the ansatz with symmetry breaking layers

When the ansatz contains symmetry-breaking layers, an optimization algorithm easily gets stuck in local minima. We here compare several different set-ups for the transverse field Ising model we have studied in Sec. III. We show results from the transverse Ising model with different initial values and using the centered and uncentered Fisher matrix in Fig. 6. We can see that the result with $\{\phi_j\}$ initialized from $\mathcal{N}(0, \sigma^2)$ and using the centered Fisher matrix is the most natural. However, when $D = 3, 5$, the results with $\{\psi_j\}$ initialized from $\mathcal{N}(2\pi/D, \sigma^2)$ show better convergence.

We have also found that using the uncentered Fisher matrix improves convergence for $D = 4$ where the centered Fisher matrix failed to find an appropriate optimum. Our results suggest that the learning landscape of the VQEs with symmetry-breaking layers is rugged, especially when the parameters are not sufficient to describe the ground state accurately.

¹F. Arute, K. Arya, R. Babbush, D. Bacon, J. C. Bardin, R. Barends, R. Biswas, S. Boixo, F. G. S. L. Brandao, D. A. Buell, and et al., “Quantum supremacy using a programmable superconducting processor,” *Nature* **574**, 505–510 (2019).

- ²J. Preskill, “Quantum Computing in the NISQ era and beyond,” *Quantum* **2**, 79 (2018).
- ³F. Pan, K. Chen, and P. Zhang, “Solving the sampling problem of the sycamore quantum circuits,” *Physical Review Letters* **129**, 090502 (2022).
- ⁴Y. Kim, A. Eddins, S. Anand, K. X. Wei, E. Van Den Berg, S. Rosenblatt, H. Nayfeh, Y. Wu, M. Zaletel, K. Temme, *et al.*, “Evidence for the utility of quantum computing before fault tolerance,” *Nature* **618**, 500–505 (2023).
- ⁵A. Peruzzo, J. McClean, P. Shadbolt, M.-H. Yung, X.-Q. Zhou, P. J. Love, A. Aspuru-Guzik, and J. L. O’Brien, “A variational eigenvalue solver on a photonic quantum processor,” *Nature communications* **5**, 1–7 (2014).
- ⁶J. R. McClean, J. Romero, R. Babbush, and A. Aspuru-Guzik, “The theory of variational hybrid quantum-classical algorithms,” *New Journal of Physics* **18**, 023023 (2016).
- ⁷M. Cerezo, A. Arrasmith, R. Babbush, S. C. Benjamin, S. Endo, K. Fujii, J. R. McClean, K. Mitarai, X. Yuan, L. Cincio, *et al.*, “Variational quantum algorithms,” *Nature Reviews Physics* **3**, 625–644 (2021).
- ⁸D. Wecker, M. B. Hastings, and M. Troyer, “Progress towards practical quantum variational algorithms,” *Physical Review A* **92**, 042303 (2015).
- ⁹S. Hadfield, Z. Wang, B. O’Gorman, E. G. Rieffel, D. Venturelli, and R. Biswas, “From the quantum approximate optimization algorithm to a quantum alternating operator ansatz,” *Algorithms* **12**, 34 (2019).
- ¹⁰E. Farhi, J. Goldstone, and S. Gutmann, “A quantum approximate optimization algorithm,” *arXiv preprint arXiv:1411.4028* (2014).
- ¹¹M. Suzuki, “Generalized Trotter’s formula and systematic approximants of exponential operators and inner derivations with applications to many-body problems,” *Communications in Mathematical Physics* **51**, 183–190 (1976).
- ¹²W. W. Ho and T. H. Hsieh, “Efficient variational simulation of non-trivial quantum states,” *SciPost Phys* **6**, 29 (2019).
- ¹³D. Wierichs, C. Gogolin, and M. Kastoryano, “Avoiding local minima in variational quantum eigensolvers with the natural gradient optimizer,” *Physical Review Research* **2**, 043246 (2020).
- ¹⁴R. Wiersema, C. Zhou, Y. de Sereville, J. F. Carrasquilla, Y. B. Kim, and H. Yuen, “Exploring entanglement and optimization within the hamiltonian variational ansatz,” *PRX Quantum* **1**, 020319 (2020).
- ¹⁵S. Bravyi, A. Kliesch, R. Koenig, and E. Tang, “Obstacles to variational quantum optimization from symmetry protection,” *Physical Review Letters* **125**, 260505 (2020).
- ¹⁶X.-G. Wen, *Quantum field theory of many-body systems: from the origin of sound to an origin of light and electrons* (OUP Oxford, 2004).
- ¹⁷B. Zeng, X. Chen, D.-L. Zhou, and X.-G. Wen, *Quantum information meets quantum matter* (Springer-Verlag New York, 2019).
- ¹⁸A. J. Beekman, L. Rademaker, and J. van Wezel, “An introduction to spontaneous symmetry breaking,” *SciPost Phys. Lect. Notes* , 11 (2019).
- ¹⁹L. Landau, “On the theory of phase transitions,” *Zh. Eksp. Teor. Fiz* **7**, 19–32 (1937).
- ²⁰P. Pfeuty, “The one-dimensional ising model with a transverse field,” *ANNALS OF PHYSICS* **57**, 79–90 (1970).
- ²¹F. D. M. Haldane, “Nonlinear field theory of large-spin heisenberg antiferromagnets: semiclassically quantized solitons of the one-dimensional easy-axis néel state,” *Physical Review Letters* **50**, 1153 (1983).
- ²²J. M. Kosterlitz and D. J. Thouless, “Ordering, metastability and phase transitions in two-dimensional systems,” *Journal of Physics C: Solid State Physics* **6**, 1181 (1973).
- ²³F. D. M. Haldane, “Nobel lecture: Topological quantum matter,” *Reviews of Modern Physics* **89**, 040502 (2017).
- ²⁴I. Affleck, T. Kennedy, E. H. Lieb, and H. Tasaki, “Rigorous results on valence-bond ground states in antiferromagnets,” *Physical Review Letters* **59**, 799 (1987).
- ²⁵T. Senthil, “Symmetry-protected topological phases of quantum matter,” *Annu. Rev. Condens. Matter Phys.* **6**, 299–324 (2015).
- ²⁶X. Chen, Z.-C. Gu, and X.-G. Wen, “Classification of gapped symmetric phases in one-dimensional spin systems,” *Physical Review B* **83**, 035107 (2011).
- ²⁷N. Schuch, D. Pérez-García, and I. Cirac, “Classifying quantum phases using matrix product states and projected entangled pair states,” *Physical Review B* **84**, 165139 (2011).
- ²⁸T. J. Osborne, “Simulating adiabatic evolution of gapped spin systems,” *Physical Review A* **75**, 032321 (2007).
- ²⁹S. Bravyi, M. B. Hastings, and S. Michalakis, “Topological quantum order: stability under local perturbations,” *Journal of mathematical physics*

- 51 (2010).
- ³⁰F. Verstraete, J. I. Cirac, J. I. Latorre, E. Rico, and M. M. Wolf, “Renormalization-group transformations on quantum states,” *Physical Review Letters* **94**, 140601 (2005).
- ³¹S. Bachmann, S. Michalakis, B. Nachtergaele, and R. Sims, “Automorphic equivalence within gapped phases of quantum lattice systems,” *Communications in Mathematical Physics* **309**, 835–871 (2012).
- ³²X. Chen, Z.-C. Gu, and X.-G. Wen, “Complete classification of one-dimensional gapped quantum phases in interacting spin systems,” *Physical Review B* **84**, 235128 (2011).
- ³³G. B. Mbeng, R. Fazio, and G. Santoro, “Quantum annealing: A journey through digitalization, control, and hybrid quantum variational schemes,” arXiv preprint arXiv:1906.08948 (2019).
- ³⁴T. Harty, D. Allcock, C. J. Ballance, L. Guidoni, H. Janacek, N. Linke, D. Stacey, and D. Lucas, “High-fidelity preparation, gates, memory, and readout of a trapped-ion quantum bit,” *Physical review letters* **113**, 220501 (2014).
- ³⁵J. P. Gaebler, T. R. Tan, Y. Lin, Y. Wan, R. Bowler, A. C. Keith, S. Glancy, K. Coakley, E. Knill, D. Leibfried, *et al.*, “High-fidelity universal gate set for $9+$ ion qubits,” *Physical review letters* **117**, 060505 (2016).
- ³⁶S. McArdle, T. Jones, S. Endo, Y. Li, S. C. Benjamin, and X. Yuan, “Variational ansatz-based quantum simulation of imaginary time evolution,” *npj Quantum Information* **5**, 1–6 (2019).
- ³⁷J. Stokes, J. Izaac, N. Killoran, and G. Carleo, “Quantum natural gradient,” *Quantum* **4**, 269 (2020).
- ³⁸L. Hackl, T. Guaita, T. Shi, J. Haegeman, E. Demler, and J. I. Cirac, “Geometry of variational methods: dynamics of closed quantum systems,” *SciPost Phys.* **9**, 48 (2020).
- ³⁹C.-Y. Park and M. J. Kastoryano, “Geometry of learning neural quantum states,” *Physical Review Research* **2** (2020), 10.1103/physrevresearch.2.023232.
- ⁴⁰G. Zonzo and S. M. Giampaolo, “ n -cluster models in a transverse magnetic field,” *Journal of Statistical Mechanics: Theory and Experiment* **2018**, 063103 (2018).
- ⁴¹W. Son, L. Amico, and V. Vedral, “Topological order in 1d cluster state protected by symmetry,” *Quantum Information Processing* **11**, 1961–1968 (2011).
- ⁴²J. R. McClean, S. Boixo, V. N. Smelyanskiy, R. Babbush, and H. Neven, “Barren plateaus in quantum neural network training landscapes,” *Nature communications* **9**, 1–6 (2018).
- ⁴³Z. Holmes, K. Sharma, M. Cerezo, and P. J. Coles, “Connecting ansatz expressibility to gradient magnitudes and barren plateaus,” *PRX Quantum* **3**, 010313 (2022).
- ⁴⁴S. S. Du, X. Zhai, B. Poczos, and A. Singh, “Gradient descent provably optimizes over-parameterized neural networks,” in *International Conference on Learning Representations* (2019).
- ⁴⁵H. Wagner and U. Schollwoeck, “Mermin-Wagner Theorem,” *Scholarpedia* **5**, 9927 (2010), revision #122055.
- ⁴⁶T. Byrnes and Y. Yamamoto, “Simulating lattice gauge theories on a quantum computer,” *Physical Review A* **73**, 022328 (2006).
- ⁴⁷H. Häffner, C. F. Roos, and R. Blatt, “Quantum computing with trapped ions,” *Physics reports* **469**, 155–203 (2008).
- ⁴⁸M. Saffman, T. G. Walker, and K. Mølmer, “Quantum information with rydberg atoms,” *Reviews of modern physics* **82**, 2313 (2010).
- ⁴⁹M. H. Devoret and R. J. Schoelkopf, “Superconducting circuits for quantum information: an outlook,” *Science* **339**, 1169–1174 (2013).
- ⁵⁰L. Henriot, L. Beguin, A. Signoles, T. Lahaye, A. Browaeys, G.-O. Raymond, and C. Jurczak, “Quantum computing with neutral atoms,” *Quantum* **4**, 327 (2020).
- ⁵¹I. Tzitrin, J. E. Bourassa, N. C. Menicucci, and K. K. Sabapathy, “Progress towards practical qubit computation using approximate Gottesman-Kitaev-Preskill codes,” *Physical Review A* **101**, 032315 (2020).
- ⁵²In contrast, all gates for the transverse-field Ising model are naturally supported by most architectures.
- ⁵³Y. Yamamoto, K. Aihara, T. Leleu, K.-i. Kawarabayashi, S. Kako, M. Fejer, K. Inoue, and H. Takesue, “Coherent Ising machines—optical neural networks operating at the quantum limit,” *npj Quantum Information* **3**, 49 (2017).
- ⁵⁴D. Stilck França and R. Garcia-Patron, “Limitations of optimization algorithms on noisy quantum devices,” *Nature Physics* **17**, 1221–1227 (2021).
- ⁵⁵C.-Y. Park, <https://github.com/chaeyeunpark/efficient-vqe-symmetry-breaking> (2021).